2016 24th International Lightning Detection Conference &
6th International Lightning Meteorology Conference
18 - 21 April | San Diego, California, USA

# Radar and Lightning Observations of a Supercell Storm on 13 June 2014 from STORM973*

*Dongxia Liu, Xiushu Qie, Yu Wang Dongfang Wang*
*Institute of Atmospheric Physics, CAS,*
*Beijing, China, 100029*
*liudx@mail.iap.ac.cn*

*Debin Su and Wenjing Xu*
*Beijing Meteorological Administrator, Beijing 100089, China,*

*Xian Xiao*
*Institute of Urban Meteorology, China Meteorology Administrator, Beijing 100089, China,*

**This study investigated the electrical and kinematic evolution of an isolated supercell storm observed on 13 June 2014. Lightning characteristics from Beijing Lightning Network (BLNet) and Doppler-derived vertical velocities, radar reflectivity, are examined during the whole life time nearly 6-h period of storm. The most striking feature of this supercell was its high percentage of cloud-to-ground (CG) lightning. At the initial stage, lightning mainly occurred in the strong radar echo, a high percentage of CG lightning was positive during this stage. Although this storm was electrically active, with maximum flash rates near 180 per minute, no CG flashes of either polarity in the stratiform region were detected at mature stage. At dissipating stage, lightning decreased sharply but with high percentage of +CG lightning. Overall, CG lightning of supercell presented early +CG and dissipating +CG mode. The charge structure of supercell inferred from the BLNET observations showed the dipole charge structure with large scale positive charge region, and the normal tripole charge distribution at the mature stage. At dissipating stage, the positive charge region in the upper level slant to stratiform region, leading to increased +CG lightning.**

***Keywords—Beijing Lightning Network; Supercell; lightning; charge structure***

## INTRODUCTION

In recent years, the networks capable of accurately measuring the total lighting, and many important results have been achieved. The LDAR Ⅱ lightning detection and ranging network upgraded after LADR (Carey et al., 2005) is comprised of an array of seven VHF antenna and receivers. A median range of accuracy of 2 km is expected at distance of 100-150 km from the center of the network. The arrival times of lightning are measured by demodulating the VHF signals into a 5-MHz base band with a center frequency of 63 MHz. The lightning mapping array (LMA) (Thomas et al., 2004) is similar to the LDAR, included six sensors operating in the frequency range of 60 to 66 MHz, with location accuracies reaching 50 m that are capable of describing the three-dimensional structure of lightning (diameter-100 km). One lightning flash produces hundreds of impulsive bursts of VHF radiation which can be measured and used to describe the structure of the lightning. SAFIR 3000 measures the phase difference of electromagnetic waves of lightning using an antenna array with a very high frequency from 110 to 118 MHz and a low frequency (LF) from300 Hz to 3 MHz (Liu et al., 2011).

Utilizing the lightning information observed by the lightning detection network, the lightning activities of different categories of convective system are investigated. Lightning and radar echo had good relationship, most of lightning occurred in the strong radar echo. With the fine lightning propagated structure, the charge structure of thunderstorm were acquired, including tripole charge structure, invert charge structure, dipole charge structure and multi charge structure. And Lightning frequency change sharply could be as an indictor of convective forecasting (Schur et al., 2009).

Lightning not only indicates the intensity and development of the convection system, but also forecast the development of storm. Studies of lightning activities combined with the dynamical or microphysical processes of thunderstorms will reveal the charge structure of a thunderstorm and provide a theoretical reference for forecasting lightning activities in severe weather (Williams et al., 1989; Qie et al., 1993). The mesocyclone region of a supercell storm had total flash rates were larger than in most other types of isolated storms (MacGorman et al. 2005). From electric-field soundings, Marshall et al., (1995) and Stolzenburg et al., (1998) investigated the charge structure of supercell, and compared charge structure in strong and weak updrafts of supercell storms. MacGorman et al., (2005) and Wiens et al., (2005) examined the electrical structure of supercell storms during STEPS, found that supercell storms presented invert charge structure, and the strong updraft had fewer vertically separated charge regions than near the rainy downdraft, and the

updraft's lowest charge was elevated higher. Weiss et al (2012) and Klumn et al. (2009) analyzed the evolution and structure of lightning in the anvils of supercell storms. They found that lightning initial within or near the stronger reflectivities of the parent storm propagated to anvil area or generated in anvil itself. Simulations of supercell storms (Ziegler and MacGorman 1994; Mansell 2000; Barthe and Pinty, 2007; Kuhlman et al., 2006) utilized electrical model simulated the charge structure of supercell storms, found that the charge structure in different supercell presented different features.

Aforementioned researches shed new light on the lightning activity of super storm that the lightning propagation and lightning location are significantly related to the charge structure distribution of thunderstorm. Due to detection accuracy limitation, it is not easy to get the good lightning information in the well-organized thunderstorms. With the established Beijing lightning network during the Dynamic-microphysical-electrical Processes in Severe Thunderstorms and Lightning Hazards (Storm973), the lightning activities and charge structure in different types of thunderstorm will be investigated deeply.

## DATA AND METHODS

### *Beijing lightning network*

The lightning data involved in this study is BLNET( Beijing Lightning Network), which including 16 sub-station, covered within covering most part of the "Jing-Jin-Ji" (Beijing-Tianjin-Hebei) metropolis zone (Figure1). The BLNET could detect total lightning information with good efficiency, which the theoretical horizontal error over the network is less than 200 m and the vertical error is less than 500 m over the network. Each station is comprised of fast electrical field change meter, slow electrical field change meter, magnetic antenna, and lightning detection antenna with very high frequency (VHF), which multi-band comprehensive observation of lightning. In order to improve the accuracy of lightning, the lightning pause are detected LF antenna at least four stations at same time. The Chan algorithm and Levenberg-Marquardt method are adopted to located lightning algorithm. In addition to locate the lightning radiation pulses in 2D or 3D in different band, the charge source neutralized by the lightning discharge can be retrieved either.

### *Lightning data*

According to the method of Cummius et al. (1998), the lightning data were filtered such that a flash event in a 10 km range within 1s was considered as a single lightning flash. Furthermore, the positive and negative polarities of return strokes were defined as +CG and −CG flashes, respectively. The location of CG lightning flash is determined by the position of return stroke. Meanwhile, distant or strong intracloud (IC) lightning flashes might be recognized as +CG flashes; therefore, +CG flashes less than 10 kA were considered as IC lightning in this study. The location algorithm and lightning efficiency of this network in details are see the results of Wang et al.(2016).

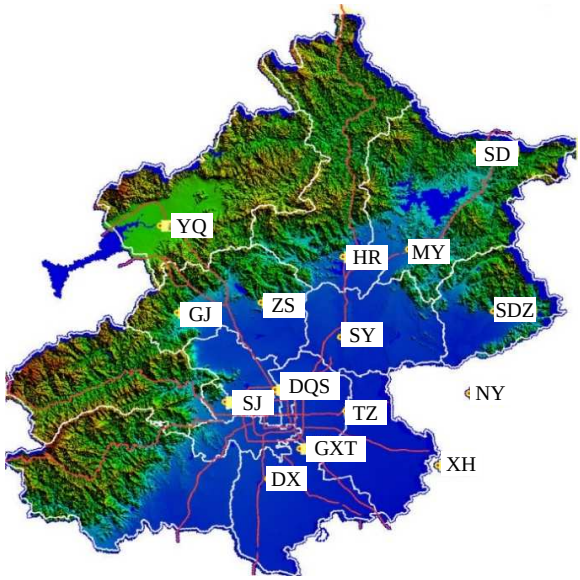


Figure 1. The topography of Beijing area with the detection stations of BLNT, including 16 sub-stations around Beijing area.

### *Radar data*

The radar data used in this study is provided from S-band Doppler radar located at 39.814° N and 116.472° E available from the Beijing Meteorological Administration. It has the 7-level elevations scan every 6 minutes and covers a range of 230 km radius.

Beside of the S-band radars, the detection network included two X-band multi-parameter radar, participated in the coordinated observations of Dynamic-microphysical-electrical Processes in Severe Thunderstorms and Lightning Hazards.

### *Meterological data*

In this study, the data form rain gauge, sounding and automatic meteorological station are also utilized to analyze the lightning activity

During the period of coordinated observation, we observed different types of thunderstorms including squall line, thunderstorm groups, super cell and hailstorm. In this study, the lightning actives of supercell are investigated by radar and lightning data.

## RESULTS

### *Case overview*

Due to the special terrain conditions of the western mountains and eastern plain, combined with low-level northerly cold and southerly warm flow, generate convective weather system frequently around Beijing area. Convection system gradually intensifies as a result of topographic forcing, and radar reflectivity is then enhanced as the system moves downslope from the mountain edges. The spatial distribution of thunderstorm occurrence indicates that southerly warm and

moist flow is forced upward by the slanted topography, generating a windward upslope effect favorable for the initiation of convective storms. In this area, there are meteorology observations including several radar stations, and weather stations, but lack of lightning detection.

A supercell happened on June 13th, 2014, moved from northeast to southeast, lasted for 8 hours with hail disaster and gust during the coordinated observations of Dynamic-microphysical-electrical Processes in Severe Thunderstorms and Lightning Hazards. This supercell, influenced by northeast cold vortex, initiated at the edge of northeastern mountain, and gradually intense and characterized as a high-precipitation supercell when it went into Beijing area, produced modest amounts of hail with surface report of large (5 cm) hailstones.

*Lightning activities in supercell*

At the initial stage, the convective system gradually formed, the amount of lightning increased sharply and +CG lightning predominated at this stage. With the thunderstorm developed, convective leading line tended to curve into circle shape and the lightning mainly occurred in the strong radar echo. At 16:42 LT (Local time), when the thunderstorm into developing stage, +CG lightning exhibited high percentage than –CG lightning. And the lightning mainly located in the strong radar echo (greater than 45 dBZ), it is proved that the BLNET lightning network has good detection efficiency. Doppler-derived updraft speed was greater than 30 $m.s^{-1}$, and the maximum radar reflectivity reached to 68 dBZ. When the main body of supercell entranced into Beijing area, amount of lightning detected during this stage. Within the thunderstorm developed into the mature stage, IC lightning and CG lightning increased sharply, the amount of lightning reached to maximum. At 17:36 LT, the strong radar echo greater than 45 dBZ presented obvious circle shape, forming a typical supercell system, although the IC lightning predominated in the whole lifetime of thunderstorm, -CG lightning increased rapidly and the ratio of +CG lightning decreased sharply. With the supercell into the dissipating stage, the circle strong radar echo disappeared, the scale and intense of radar are all decreased. Lightning distribution slanted to the stratiform region and dominated with +CG lightning. Lightning frequency gradually declined, but still with high percentage of +CG lightning. During the whole life time of supercell, the lightning activity presented +CG lightning predominated at early and later time.

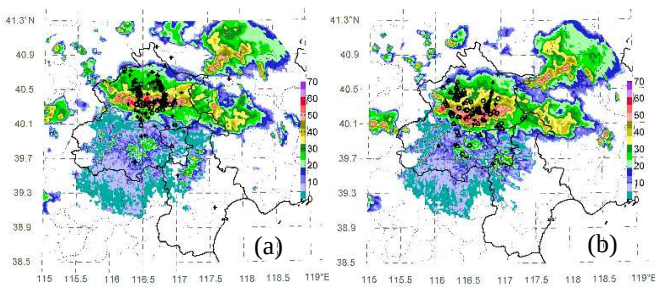


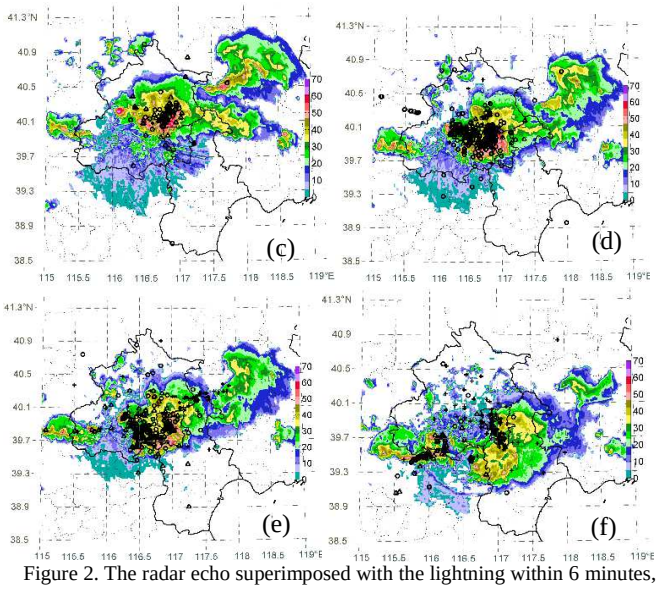


Figure 2. The radar echo superimposed with the lightning within 6 minutes, black circle stands for IC lightning, black triangle stands for –CG lightning, "+"stands for + CG lightning. (a)16:24 , (b) 16:42,(c)17:00, (d) 17:36, (e)17:54 (f) 18:48 LT.

Figure 3 showed lightning frequency within 5 minutes of supercell. During the early time of supercell (16:00-17:00 LT), the lightning gradually increased and the percentage of +CG larger than –CG lightning. With the supercell came into the developing stage, lightning frequency increased dramatically, especially IC lightning. At the mature stage, both IC lightning and CG lightning reach to the maximum, corresponding to the strong radar echo formed into round shape. And then the percentage of IC lightning gradually decreased and the percentage of CG lightning increased, particularly the –CG lightning. When the supercell into dissipating stage, the lightning frequency gradually decreased, but with high percentage of +CG lightning.

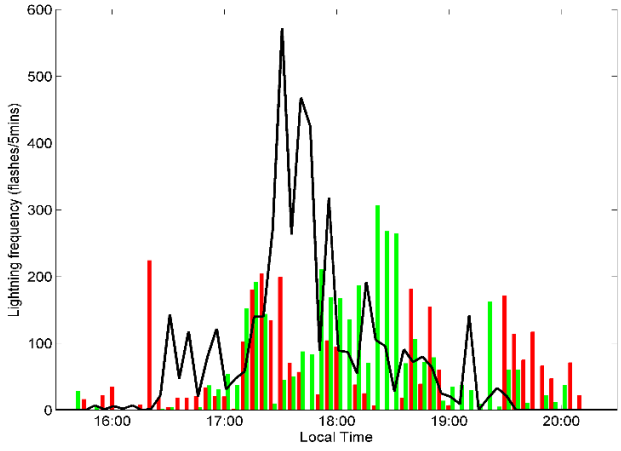


Figure 3 lightning frequency within 5 minutes, green bar stands for –CG lightning, red bar stands for + CG lightning.

*Vertical distribution of lightning*

Figure 4 show the IC lightning pulses superimposed on radar cross section during mature stage. Because we focused on the vertical lightning distributions, the height of lightning pulse with zero is not considered. At 17:24, lightning pulse mainly concentrated in the transition zone, which connected the leading convective and trailing stratiform region. IC flashes in the strong radar echo (>45 dBZ) reached to higher level of 8 km, then sloped down to the stratiform region through transition zone. At the lower level (about 4 km)of strong radar echo, it is clear to see that the lightning channel initiated from the core of radar echo and propagated down to the ground. In the trailing stratiform region, lighting pulses scattered in the large scale of secondary maximum radar echo. Carey et al., (2005) using the lightning radiation sources, analyzed charge structure in a MCS and pointed out lightning radiation reached to maximum in convective region and slant to stratiform region through transition area. At 17:36, the strong radar echo extend to higher level and lightning pulses reach to upper level. In the transition area, it is can be seen the lightning path from convective region to stratiform region. The lighting pulses concentrated in the great gradient of radar reflectivity.

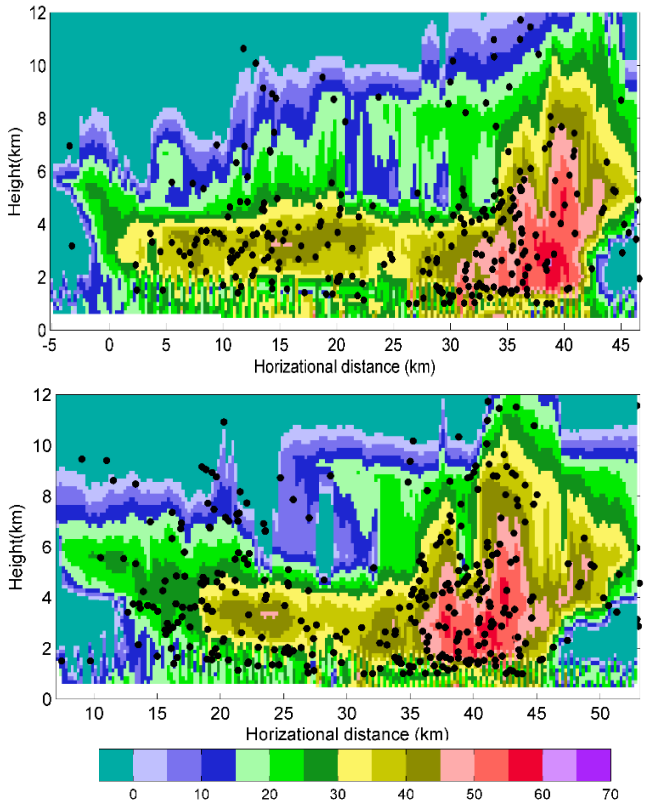


Figure 4. Radar cross-section and lightning pulses distribution within 6 minutes, (a) 17:24 ,(b) 17:36

## CONCLUSION

Utilzed a lightning network of BLNET, the lightning activity of supercell is investigated. +CG lightning take a high percentage of CG lighting, particularly in the early and later time. Plausible explanations for the +CG lightning occurring in supercell include tilted charge structure, enhanced lower charge region, and inverted charge structure (Marshall et al., 1995; Rust et al., 2005). MacGorman et al. (2005) observed inverted-polarity IC and +CG flashes in a supercell were caused by inverted-polarity storm structure, and they assume possibly due to a larger than usual rime accretion rate for graupel in a strong updraft. In this study, -CG lightning predominated at the mature stage, discharge by main negative region. The distribution of lightning pulses demonstrated that one part of the lightning initiated from convective region to stratiform region through transition area, another part of pulses generated in the stratiform region by itself. In this case, the +CG flashes in supercell might be caused by the horizontal upper-level positive charge from the convective region to the stratiform region by the advection flow along the convective region. Without less sheltering from lower negative charge region, the upper positive charge in stratiform region discharged directly to the ground. Future works will combine model simulation with observation to investigate the lightning activity of supercell in greater detail.

## ACKNOWLEDGMENT

This study is supported by the National Key Basic Research Program of China (No. 2014CB441401). The Beijing Meteorological Administration is appreciated for providing the radar data. Thanks for the effort of all the people participated in coordinated observations of Dynamic-microphysical-electrical Processes in Severe Thunderstorms and Lightning Hazards.

## REFERENCES

Barthe, C., and J.-P. Pinty (2007), Simulation of a supercellular storm using a three-dimensional mesoscale model with an explicit lightning flash scheme, J. Geophys. Res., 112, D06210, doi:10.1029/2006JD007484.

Carey, L. D., M. J. Murphy, T. L. McCormick, and N. W. S. Demetriades, (2005), Lightning location relative to storm structure in a leading-line, trailing-stratiform mesoscale convective system, J. Geophys. Res., 110, D03105, doi:10.1029/2003JD004371.

Cummins, K. L., M. J. Murphy, E. A. Bardo, W. L. Hiscox, R. B. Pyle, and A. E. Pifer, (1998), A combined TOAA/MDF technology upgrade of the U.S. National Lightning Detection Network. *J. Geophys. Res.*, **103,** 9035–9044.

Kuhlman, K. M., C. L. Zielger, E. R. Mansell, D. R. MacGorman, and J. M. Straka, (2006), Numerically simulated electrification and lightning of the 29 June 2000 STEPS supercell storm. Mon. Wea. Rev., 134, 2734–2757.

Kuhlman, , K. M., D. MacGorman, M. Biggerstaff, and P. Krehbiel, (2009), Lightning initiation in the anvils of two supercell storms. Geophys. Res. Lett., 36, L07802, doi:10.1029/2008GL036650.

Liu, D. X., X. S. Qie, and Y. J. Xiong, (2011), Evolution of the total lightning structure in a leading-line, trailing stratiform mesoscale convective system over Beijing. *Adv. Atmos. Sci.*, 28, 1-13.

MacGorman, D.R., W.D. Rust, P. Krehbiel, W. Rison, E. Bruning, and K. Wiens, (2005), The electrical structure of two supercell storms during STEPS. Mon. Wea.Rev., 2583-2607

Mansell, E. R., (2000), Electrification and lightning in simulated supercell and non-supercell thunderstorms. Ph.D. dissertation, University of Oklahoma, Norman

Marshall, T., W. Rust, W. Winn, and K. Gilbert, (1989), Electrical structure in two thunderstorm anvil clouds. J. Geophys. Res., 94, 2171–2181.

Qie X. S., C. M. Guo, M. H. Yan, G. S. Zhang, (1993), Lightning data and study of thunderstorm nowcasting, ACTA Meteorologica Sinica, 7 (2), 244-256.

Rust, W. D., D. R. MacGorman, E. C. Bruning, S. A. Weiss, P. R. Krehbiel, R. J. Thomas, W. Rison, T. Hamlin, J. Harlin, (2005), Inverted-polarity electrical structures in thunderstorms in the Severe Thunderstorm Electrification and Precipitation Study (STEPS). *Atmos. Res.*, 76, 247-271.

Schultz, Christopher J., Walter A. Petersen, Lawrence D. Carey (2010), Lightning and Severe Weather: A Comparison between Total and Cloud-to-Ground Lightning Trends. *Wea. forecasting*, 26, 744-755.

Stolzenburg,M., W. D. Rust, and T. C. Marshall, (1998), Electrical structure in thunderstorm convective regions. 2. Isolated storms. J. Geophys. Res., 103, 14 079–14 096.

Thomas, R. J., P. R. Krehbiel, W. Rison, S. J. Hunyady, W. P. Winn, T. Hamlin, and J. Harlin, (2004), Accuracy of the lightning mapping array. J. Geophys. Res., 109, D14207, doi:10.1029/ 2004JD004549.

Wang, Y., X. Qie, D. Wang, M. Liu, (2016), Beijing Lightning Network (BLNET): A research and operational system for comprehensive lightning detection, Atmos. Res., 171:121‑132

Weiss, S. A., D. R. MacGorman, and K. M. Calhoun, (2012), Lightning in the Anvils of Supercell Thunderstorms. Mon. Wea. Rev., 140, 2064–2079

Wiens, K. C., S. A. Rutledge, and S. A. Tessendorf, (2005), The 29 June 2000 supercell observed during STEPS. Part II: Lightning and charge structure. J. Atmos. Sci., 62, 4151–4177.

Williams, E. R., (1989), The tripole structure of thunderstorms. J. Geophys. Res., 94, 13 151–13 167.

Ziegler, C. L., and D. R. MacGorman, (1994), Observed lightning morphology relative to modeled space charge and electric field distributions in a tornadic storm. J. Atmos. Sci., 51, 833– 851.